Thickness dependence of leakage currents in high-permittivity thin films

Herbert Schroeder[a] and Sam Schmitz[b]
Institut für Elektrokeramische Materialien im Institut für Festkörperforschung and CNI-Center of Nanoelectronic Systems for Information Technology, Forschungszentrum Jülich GmbH, D-52425 Jülich, Germany

(Received 2 July 2003; accepted 26 September 2003)

The leakage current through high-permittivity perovskite thin films in the nanometer range is of great technological interest because of the possible applications of these insulating films in future submicroelectronic devices such as dielectrics in Gbit dynamic random access memories or gate oxides in metal–oxide–semiconductor field-effect transistors. The experimental result of decreasing leakage current with decreasing thickness of the dielectric for the same externally applied field can be described by using a model combining thermionic emission at the electrode/dielectric interface and a low-mobility, high-permittivity dielectric with low-permittivity layers at the interfaces, the so-called dead layers. © *2003 American Institute of Physics.* [DOI: 10.1063/1.1629141]

Thin films of high-permittivity perovskite materials, represented by the ''model'' alloys $SrTiO_3$ (STO) and $(Ba,Sr)TiO_3$ (BST), are discussed as substitutes for low-permittivity Si-oxide/-nitride (ON) films in future ultra-large-scale integrated electronic circuits, e.g., as dielectrics in the capacitor of Gb-generation dynamic random access memory (DRAM) cells[1] or as gate oxides in metal–oxide–semiconductor field-effect transistors (MOSFETs).[2] One of the reasons for seeking replacements for the very thin ON films is the unacceptably high leakage current through these films resulting in charge, and thus in information loss in the DRAM or in a too high zero current of the MOSFET in the ''off'' state. Therefore, the understanding of the leakage mechanisms in perovskite materials also has an important technological aspect, especially the question of how the leakage current density in the these thin films will behave in the case of decreasing thickness.

Only a few results have been published in the literature on systematic investigations of the thickness dependence of the leakage current in perovskite thin dielectric films.[3] Recently, some very interesting experimental results have been published,[4–9] all showing that the leakage current density at a fixed mean applied field, $\langle E\rangle = U_{\mathrm{appl}}/t$, decreases with decreasing dielectric thickness, t, in planar metal–insulator–metal capacitors. U_{appl} is the externally applied voltage. All the groups used Pt for the metal electrodes and BST (with different compositions and deposition methods) for the dielectrics. An example is shown in Fig. 1. The leakage current density, j, is plotted versus mean applied field, $\langle E\rangle$, for samples with different dielectric thicknesses, in this case between 30 and 150 nm. At constant $\langle E\rangle$ the leakage current density is clearly much lower for smaller thickness. For example, at a field of 900 kV/cm the leakage current density is about 0.1 A/cm^2 for the 150-nm-thick sample, but less than 10^{-5} A/cm^2 for the 30-nm-thick sample. This means more than four orders of magnitude of current reduction for the thinnest sample.

Some of the experiments mentioned[5–7] were performed in our laboratory with $Pt/Ba_{0.7}Sr_{0.3}Ti\,O_3/Pt$ capacitors. The BST is polycrystalline with columnar grains. More details of the metal–organic chemical vapor deposition conditions and resulting microstructure as well as chemical characterization and experimental setup are published in Refs. 5–7 and 9. The dielectric thickness was varied between 14 and 111 nm, the leakage current experiments were usually performed at ambient temperature [room temperature (RT)] with applied voltages of up to 3–7 V. Some characteristic results are plotted in Fig. 2(a) versus the square root of the applied field, i.e., a ''Schottky'' plot. Using this plot most of the curves are linear over a wide range. Clearly, the leakage is lowest for the thinnest and highest for the thickest film at all fields.

In addition to the experiments at RT, we also investigated the thickness dependence of the leakage current at higher temperatures. It is worth noting that the minimum of the current–time curve (measured for 1000 s) was always used for the leakage current. An example is shown in Fig. 2(b) for the test series at 425 K, which is probably above the highest temperature for the applications mentioned. The largest applied voltages were between 2 and 4 V. At a field of 300 kV/cm, for which all curves are in the almost straight region in this plot, the difference is more than three orders of magnitude between the thickest and thinnest specimens. The curves for the samples with thicknesses between the thickest and thinnest specimens have leakage currents in between, but their order is not as perfect for all fields.

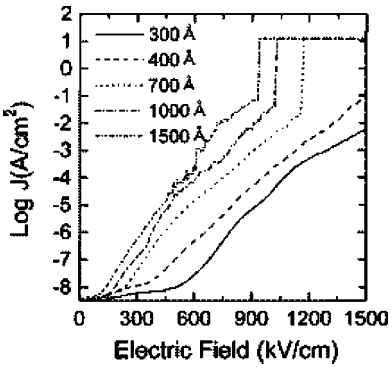

FIG. 1. Leakage current density j vs applied electrical field E for Pt/BST/Pt planar capacitor structures with different dielectric thickness (30–150 nm) (from Ref. 4).

[a]Electronic mail: he.schroeder@fz-juelich.de
[b]Present address: Stiftung Caesar, D-53175 Bonn, Germany.

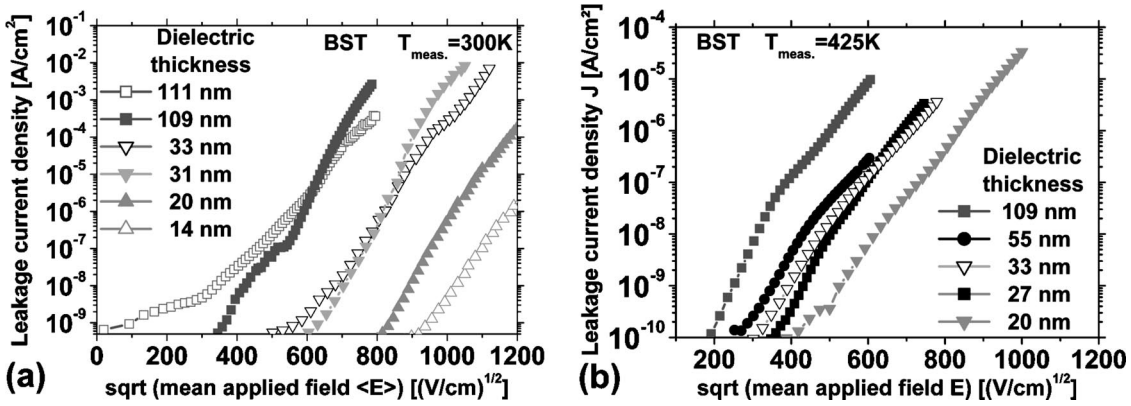

FIG. 2. Leakage current density j vs square root of the applied electrical field $\langle E\rangle^{1/2}$, for Pt/BST/Pt planar capacitor structures with different dielectric thicknesses. (a) 14–111 nm; $T=300$ K; full symbols: Ti rich, open symbols: (Ba,Sr) rich (after Ref. 6). (b) 20–109 nm; $T=425$ K; all Ti rich.

This behavior of decreasing leakage current with decreasing dielectric thickness has been observed for a wide range of Pt/BST/Pt capacitors with different deposition methods and parameters as well as for STO dielectrics,[10] although there are certain differences in the absolute values of the current densities and the form of the curves, which may be associated with the differences in material or treatment. Additionally, nearly all curves show large linear portions in the Schottky plot.

We recently published a model and corresponding simulation calculations[11] that quantitatively describe the current–field curve of the 55-nm-thick specimen in Fig. 2(b). The same model can also predict the measured thickness dependence of the current–field curves presented in Figs. 1 and 2 as shown below. The major components of that model will be outlined briefly.

The dielectric film of thickness t between the (Pt) electrodes consists of three layers: the high-permittivity film, the ''bulk'' (thickness $t-2a$; permittivity $\varepsilon_{\text{film}}$), and a thin layer at each electrode/dielectric interface of thickness $a \ll t$ with a low-permittivity $\varepsilon_I \ll \varepsilon_{\text{film}}$ (for convenience, the identical ''dead layers'' are assumed). All other properties (band-gap energy, mobility, defect densities, etc.) are identical throughout the film. It is described as a linear dielectric, and symmetrical electrodes are assumed. For the internal interface dead layer/dielectric film at $x=a$ and $x=t-a$, the steadiness of the dielectric displacement, $D(x)$, is used.

As usual, within the dielectric, both the Poisson equation and the continuity equation with drift and diffusion terms have to be solved in the three regions of different ε_r. For the three necessary boundary conditions we used the two barrier heights at the electrodes for the electric potential energy at the metal interfaces and the externally applied voltage (defined as the difference of the Fermi levels in the electrodes) connected to the sum of the potential drop (integral of the electrical field) inside the dielectric and a possible diffusion potential. Additional ''boundary'' conditions are used to describe the (electron) carrier injection from one metal electrode (cathode) into the dielectric and the carrier collection (i.e., recombination) at the other electrode, respectively, as suggested by the recombination velocity approach by Crowell *et al.*[12,13] These latter conditions lead, first, to a nonequilibrium description of the current (quasi-Fermi level, Imref) and, second, to a current limitation by the injection/recombination process, in this case electron injection over the barrier reduced by the Schottky lowering.

The differential equations cannot be solved analytically for the general case, but the resulting current density, j, follows an equation similar to that in the textbook by Sze,[14] also used by Baniecki *et al.*,[15] except for the last term in the denominator:

$$j=\frac{e_0 v_R N_C \exp(-e_0\Phi_{B,\text{cath}}^{\text{eff}}/kT)\{\exp(e_0U/kT)-1\}}{1+\dfrac{v_R}{v_D}+\dfrac{n_{0,\text{cath}}(x\approx 0)}{n_{0,\text{anode}}(x\approx d)}\exp(e_0U/kT)}. \tag{1}$$

e_0 is the elementary charge; $v_R=A^*T^2/e_0N_C$ is a recombination velocity;[12–14] N_C is the effective density of states in the conduction band; A^* the effective Richardson constant, i.e., the free electron value of 120 A/cm^2 K^2 possibly corrected by the effective electron mass (quantum-mechanical reflections are neglected); T the absolute temperature; k the Boltzmann constant, $e_0\Phi_{B,\text{cath}}^{\text{eff}}$ is the effective barrier height at the injecting electrode (cathode for $U<0$), including the Schottky lowering, which is dependent on the square root of the field $E(x\approx 0)$; and U is the applied voltage (<0 for the cases shown). $n_{0,\text{cath}}$ and $n_{0,\text{anode}}$ are the effective electron concentrations at the electrode interfaces, respectively:

$$n_{0,\text{cath or anode}}=N_C\exp(-e_0\Phi_{B,\text{cath or anode}}^{\text{eff}}/kT). \tag{2}$$

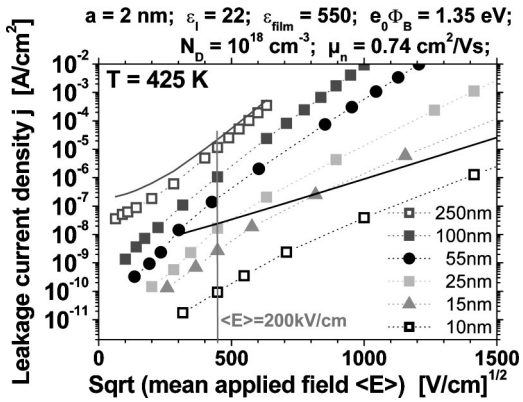

FIG. 3. Simulation data of leakage current density j vs square root of the applied electrical field, $\langle E\rangle^{1/2}$, for different dielectric thicknesses (10–250 nm). The full curves represent the Schottky injection limit for the thinnest and thickest samples, respectively.

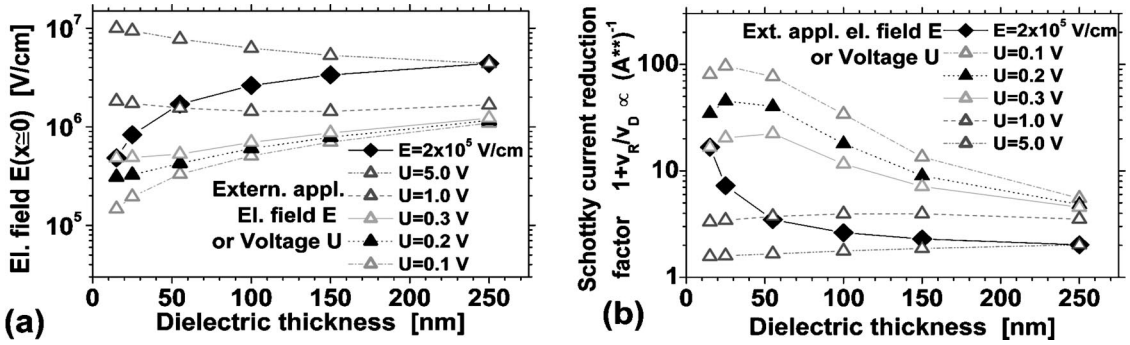

FIG. 4. Simulated thickness dependence of (a) electric field $E(x\cong 0)$ at the injecting electrode and (b) the reduction factor for the Schottky injection current due to current limitation by the dielectric film conduction. (This factor is proportional to the inverse of the effective Richardson constant, A^{**}.)

v_D is an effective ''diffusion'' velocity,[12–14] which cannot be calculated analytically for the general case:

$$(v_D)^{-1}=\frac{e_0}{\mu_n kT}\int_{x\approx 0}^{x\approx d} dx \exp\left\{-\frac{e_0}{kT}[\Phi(x\approx 0)-\Phi(x)]\right\}. \tag{3}$$

$\Phi(x)$ is the electric potential within the dielectric and μ_n is the electron mobility.

Figure 3 presents the results of the finite difference method calculations of this model for the current density versus the applied electric field for various dielectric thicknesses at $T=425$ K, once again as a Schottky plot. The parameters used are given in Fig. 3. Only the donor density, N_D, the equilibrium barrier height, Φ_B, and the ratio of dead layer thickness to the dead layer permittivity (a/ε_I) are adjustable parameters. For the fitting of the 55 nm sample in Fig. 2(b) slightly different values were used.[11] Clearly the currents are smallest for the thinnest (10 nm) and highest for the thickest (250 nm) samples. This order is true for all applied fields. At the applied field of 200 kV/cm, the current ratio between the 15 and 100 nm samples is, for example, 500 compared to about 1000 in Fig. 2(b) for the 20 and 109 nm samples at the same field.

The thickness dependence of the terms in Eq. (1) will be discussed. The numerator represents the Schottky current of two back-to-back Schottky diodes. For $e_0U\gg kT$ this value approaches the usual Schottky injection current limit. This already is realized at lower fields for thicker samples (as $U=Et$). The main factor in the Schottky current is the Schottky lowering in the effective barrier height connected to $[E(x\approx 0)]^{1/2}$. Its thickness dependence is shown in Fig. 4(a) for several cases calculated with the same parameter set as in Fig. 3. At constant field $\langle E\rangle=2\times 10^5$, the enhancement factor of $E(x\approx 0)$ compared to $\langle E\rangle$ is more than 2 for 10 nm and more than 20 for 250 nm, leading to much enhanced Schottky current limits for thicker samples (see Fig. 3). This thickness dependence is observed for all fields and is due to the field redistribution because of the dead layers. For constant voltage the dependence is different: at 1 V (roughly corresponding to the voltage in DRAM applications) $E(x\approx 0)$ is nearly independent. At smaller voltages the model shows the thinner the sample, the lower the Schottky limit, and at larger voltages the situation is reversed.

The Schottky injection current limit, the numerator in Eq. (1), may be reduced by ''bulk'' properties, e.g., the electron mobility. This is expressed in the denominator. Only if the denominator approaches unity, is the current interface limited. This holds for $v_D\gg v_R$ (the third term is negligible for most cases). Due to the low mobility in BST, usually, $v_D(\propto\mu)\ll v_R$, i.e., there is *always a reduction factor* compared to the (Schottky) current limit. Hence, the *current is bulk limited*. This is demonstrated in Fig. 4(b). In case of constant field conditions the reduction factor increases with decreasing thickness, which is true for all fields. At constant thickness it increases with decreasing voltage. The factor is much larger for thinner samples, up to 100 for the thinnest samples shown. For large voltages ($U\geqslant 1$ V), the thickness dependence is small, for smaller voltages ($U<1$ V) the reduction factor is in favor of thinner samples, i.e., smaller leakage.

In conclusion, the experimental observation of decreasing leakage currents in Pt/BST/Pt capacitors with decreasing dielectric thickness can be modeled by bulk-limited conduction with dead layers at the electrode interfaces and interface injection as boundary conditions.

[1] D. E. Kotecki, J. D. Baniecki, H. Shen, R. B. Laibowitz, K. L. Saenger, J. J. Lian, T. M. Shaw, S. D. Athavale, C. Cabral, P. R. Duncombe, M. Gutsche, G. Kunkel, Y.-J. Park, Y.-Y. Wang, and R. Wise, IBM J. Res. Dev. **43**, 367 (1999).
[2] R. A. McKee, F. J. Walker, and M. F. Chisholm, Phys. Rev. Lett. **81**, 3014 (1998).
[3] W. Dietz, M. Schumacher, R. Waser, S. K. Streiffer, C. Basceri, and A. I. Kingon, J. Appl. Phys. **82**, 2359 (1997).
[4] J. C. Shin, J. Park, C. S. Hwang, and H. J. Kim, J. Appl. Phys. **86**, 506 (1999).
[5] F. Fitsilis, S. Regnery, P. Ehrhart, R. Waser, F. Schienle, M. Schumacher, and H. Juergensen, Integr. Ferroelectr. **38**, 211 (2001).
[6] P. Ehrhart, F. Fitsilis, S. Regnery, R. Waser, F. Schienle, M. Schumacher, H. Juergensen, and W. Krumpen, Integr. Ferroelectr. **45**, 59 (2002).
[7] S. Regnery, Y. Ding, P. Ehrhart, F. Fitsilis, C. L. Jia, K. Szot, R. Waser, F. Schienle, M. Schumacher, and T. McEntee, Mater. Res. Soc. Symp. Proc. **748**, U15.6.1 (2003).
[8] K. H. Ahn, S. S. Kim, and S. Baik, J. Appl. Phys. **93**, 1725 (2003).
[9] Y. Takeshima, K. Tanaka, and Y. Takabe, Jpn. J. Appl. Phys., Part 1 **39**, 5389 (2000).
[10] S. Schmitz, Ph.D. thesis RWTH Forschungszentrum Jülich, Germany (2002); F. Fitsilis, Ph.D. thesis RWTH Forschungszentrum Jülich, Germany (2002).
[11] H. Schroeder, S. Schmitz, and P. Meuffels, Appl. Phys. Lett. **82**, 781 (2003).
[12] C. R. Crowell and S. M. Sze, Solid-State Electron. **9**, 1035 (1966).
[13] C. R. Crowell and M. Beguwala, Solid-State Electron. **14**, 1149 (1971).
[14] S. M. Sze, *Physics of Semiconductor Devices*, 2nd ed. (Wiley, New York, 1981).
[15] J. D. Baniecki, R. B. Laibowitz, T. M. Shaw, C. Parks, J. Lian, H. Xu, and Q. Y. Ma, J. Appl. Phys. **89**, 2873 (2001).